A FRACTIONAL-STEP METHOD FOR THE INCOMPRESSIBLE NAVIER–STOKES EQUATIONS RELATED TO A PREDICTOR–MULTICORRECTOR ALGORITHM

J. BLASCO, R. CODINA AND A. HUERTA*

E.T.S. Enginyers de Camins, Universitat Politècnica de Catalunya, c/ Gran Capità s/n, 08034 Barcelona, Spain

SUMMARY

An implicit fractional-step method for the numerical solution of the time-dependent incompressible Navier–Stokes equations in primitive variables is studied in this paper. The method, which is first-order-accurate in the time step, is shown to converge to an exact solution of the equations. By adequately splitting the viscous term, it allows the enforcement of full Dirichlet boundary conditions on the velocity in all substeps of the scheme, unlike standard projection methods. The consideration of this method was actually motivated by the study of a well-known predictor–multicorrector algorithm, when this is applied to the incompressible Navier–Stokes equations. A new derivation of the algorithm in a general setting is provided, showing in what sense it can also be understood as a fractional-step method; this justifies, in particular, why the original boundary conditions of the problem can be enforced in this algorithm. Two different finite element interpolations are considered for the space discretization, and numerical results obtained with them for standard benchmark cases are presented. © 1998 John Wiley & Sons, Ltd.

KEY WORDS: incompressible Navier–Stokes equations; finite elements; fractional-step methods; predictor–multicorrector algorithm; convergence analysis

1. INTRODUCTION

Since the origin of computational fluid dynamics in the 1960s, many numerical schemes have been developed for the approximation of viscous, incompressible flow equations. Among them, several fractional-step projection methods can be found. This category, originated independently by Chorin [1] and Temam [2], comprises methods developed under different ideas: fractional-step or splitting methods for evolution equations (see [3] for a comprehensive study of them); methods based on a projection onto a space of solenoidal vector fields [4], and others, such as pressure correction or velocity correction methods ([5], for instance), or recently, even approximate matrix factorization methods [6,7].

A typical derivation of a fractional-step method from the original unsteady incompressible Navier–Stokes equations can proceed in two different ways. On the one hand, a time discretization can be performed first, followed by a space discretization. When this approach is adopted, a controversy arises about what boundary conditions are to be imposed at each

* Correspondence to: E.T.S. Enginyers de Camins, Universitat Politècnica de Catalunya, c/ Gran Capità s/n, 08034 Barcelona, Spain.

step, so that the intermediate semi-discrete problems are well-posed. In particular, in most projection methods, only the normal component of the velocity boundary condition is imposed in the incompressibility step [8]. This fact, together with the need to impose unphysical boundary conditions on the pressure, can generate a numerical boundary layer [9–12]. On the other hand, when a space discretization is performed prior to a fractional-step time discretization of the resulting system of ordinary differential equations, boundary conditions are fixed from the start. However, proceeding this way results in a loss of generality.

Fractional-step projection methods have been used together with different space discretizations: finite difference [1,13–16], finite element [5,17–20] and spectral methods [21]. One important feature of each fractional-step method is the order of the overall scheme with respect to the time discretization. Most methods are first-order-accurate, but some second-order methods have also been developed [13,14].

An implicit fractional-step method is studied in this paper. A time-discretized form of the equations is presented first, which is shown to be well-posed. Full velocity boundary conditions are imposed in both phases of the scheme. A modified scheme, accounting for pressure correction, is also introduced.

Convergence of the method to a solution of the continuous problem when the time step tends to zero is proved. Both the intermediate and the end-of-step velocities are shown to converge in the space $H_0^1(\Omega)$, whereas in the original projection method of Temam, the end-of-step velocities only converge in $L^2(\Omega)$ (due to the wrong boundary conditions they satisfy). The overall algorithm is first-order-accurate in time for the velocity solution. As will be shown numerically, it is also first-order-accurate for the pressure. In Reference [22], the authors provide some error estimates that prove this first-order accuracy of the method, both with and without pressure correction.

The authors also present an iterative scheme for the solution of the fully discrete version of the method, in which each iteration consists of the solution of two diagonal systems and a system with a symmetric positive (semi-) definite matrix that is the same for all the iterations and time steps.

Based on the method just introduced, an iterative predictor–multicorrector algorithm, designed by Hughes and co-workers [23] and extensively used in the 1980s, especially in the context of fluid–structure interactions [24], is redeveloped here in a semi-discrete setting, within the context of fractional-step methods. The algorithm was suspected of having a bearing with these kind of methods but no rigorous proof of this fact was available. The classical derivation of the predictor–multicorrector algorithm consists of discretizing the Navier–Strokes equations in space by a finite element interpolation, and then applying a time advancement scheme to the resulting system of ordinary differential equations. A non-linear system of equations needs to be solved at every time step, and this is achieved by an iterative process. Each iteration of the scheme is classically decomposed into two phases; here it will be shown that this decomposition is performed in a fractional-step way. One can thus reinterpret this algorithm as a *fractional iteration* scheme. The possibility of imposing the original boundary conditions in both phases is justified by the relationship established with the present fractional-step method.

A bilinear velocity, constant pressure finite element interpolation, or $Q_1 P_0$ element, is classically used for the space variables when implementing this algorithm. This is compared here with a biquadratic velocity, linear pressure ($Q_2 P_1$) element, which turns out to be better suited for this algorithm since it satisfies the discrete *inf–sup* condition.

The paper is organized as follows: Section 2 introduces the problem to be solved, the functional setting for it and the notation used in this paper. In Section 3, the fractional-step

method, which depends on a free parameter $\theta > 0$, is studied and compared with other existing fractional-step methods. Convergence of the method for the fully implicit case $\theta = 1$ is stated in Section 4. Two different finite element interpolations of the method are considered in Section 5, together with some computational aspects. The formal derivation of the predictor–multicorrector algorithm as a fractional-step iterative method is given in Section 6. Finally, some numerical results obtained with both the present fractional-step method and the predictor–multicorrector algorithm are shown in Section 7, which confirm their accuracy properties and ability to solve both steady and unsteady problems.

2. PROBLEM STATEMENT AND NOTATION

The evolution of viscous, incompressible fluid flow in a bounded domain $\Omega \subset \mathbb{R}^d$ ($d = 2, 3$) is governed, in the primitive variable formulation, by the unsteady, incompressible Navier–Stokes equations:

$$\frac{\partial u}{\partial t} + (u \cdot \nabla)u + \nabla p - v\nabla^2 u = f, \tag{1}$$

$$\operatorname{div} u = 0, \tag{2}$$

on $\Omega \times (0, T)$, where $u(x, t) \in \mathbb{R}^d$ is the fluid velocity at position $x \in \Omega$ and time $t \in (0, T)$ (with $T > 0$ given), $p(x, t) \in \mathbb{R}$ is the fluid kinematic pressure, $v > 0$ is the kinematic viscosity, $f(x, t)$ is an external force, ∇ is the gradient operator and ∇^2 is the Laplacian operator.

Equation (1) is formally equivalent to its dimensionless form, provided $v = 1/Re$, Re being the fluid's Reynolds number. Boundary conditions have to be given to complete the equation system (1)–(2). For the sake of simplicity, only homogeneous Dirichlet-type boundary conditions are considered here:

$$u(x, t) = 0, \quad (x, t) \in \Gamma \times (0, T),$$

where the boundary $\Gamma = \partial\Omega$ is assumed to be Lipschitz continuous. However, this study can be extended to more general boundary conditions. An initial condition must also be specified for the velocity:

$$u(x, 0) = u^0(x), \quad x \in \Omega,$$

whereas no boundary or initial conditions need be specified for the pressure. The study of the above equations of motion requires the following Hilbert spaces (see [25]): $L^2(\Omega)$, equipped with the usual scalar product (u, v) and norm $|u| = (u, u)^{1/2}$; the quotient space $L_0^2(\Omega) = L^2(\Omega)/\mathbb{R}$, in the case of Dirichlet-type boundary conditions only, since the pressure term p in Equation (1) is then determined up to an additive constant; the space $H^1(\Omega)$, whose scalar product and norm are denoted by $(u, v)_1 = (u, v) + (\nabla u, \nabla v)$ and $\|u\|_1 = (u, u)_1^{1/2}$ respectively.

The space $H^1(\Omega)$ contains a closed subspace $H_0^1(\Omega)$ made up with functions that vanish at the boundary of Ω. The Poincaré–Friedrich inequality:

$$d_0(\nabla u, \nabla u)^{1/2} \geq (u, u)^{1/2}, \quad \forall u \in H_0^1(\Omega), \tag{3}$$

with $d_0 > 0$ a constant, ensures that $\|u\| = (\nabla u, \nabla v)^{1/2}$ is a norm on $H_0^1(\Omega)$, is equivalent to the norm induced by $H^1(\Omega)$. The scalar product in $H_0^1(\Omega)$ is, then, $((u, v)) = (\nabla u, \nabla v)$. The dual space of $H_0^1(\Omega)$ is denoted by $H^{-1}(\Omega)$; the duality pairing between these spaces is denoted by $\langle , \rangle$. All these definitions and results carry over to d-dimensional vector valued function spaces.

Due to the incompressibility condition (2), closed subspaces of solenoidal vector fields of these Hilbert spaces are also needed. Thus, in the standard notation, one defines:

$$H = \{u \in (L^2(\Omega))^d / \exists \, \text{div} \, u = 0 \in L^2(\Omega), \, n \cdot u|_\Gamma = 0\},$$

$$V = \{u \in (H_0^1(\Omega))^d / \text{div} \, u = 0 \in L^2(\Omega)\}.$$

3. FRACTIONAL-STEP METHOD

One way of discretizing Equations (1) and (2) in time is by fractional-step methods, in which the time advancement is decomposed into a sequence of (generally two) steps. The following class of 2-step methods is considered here:

3.1. First step

The first step of the method, which includes viscous and convective effects, consists of finding, given $u^n \in V$, an intermediate velocity $u^{n+1/2}$ such that:

$$\frac{u^{n+1/2} - u^n}{\Delta t} - \theta v \nabla^2 u^{n+1/2} - (1 - \theta) v \nabla^2 u^n + (u^n \cdot \nabla) u^{n+1/2} = \bar{f}^n, \tag{4}$$

$$u^{n+1/2}|_\Gamma = 0, \tag{5}$$

where $\Delta t > 0$ is the time step, θ is a parameter such that $0 < \theta \leq 1$ and the superscript n denotes the time level $t_n = n\Delta t$. The approximation of the non-linear term may take other forms; the semi-implicit approximation adopted here is taken form [26]. As for the approximation of the force term, one defines, following [4], $\bar{f}^n$ as the time average of f in $[t_n, t_{n+1}]$.

This first step of this method can be thought of as a linearized Burger's problem. Equations (4) and (5) can be written in weak form as $\tilde{a}_\theta(u^{n+1/2}, v) = l_0(v)$, $\forall v \in (H_0^1(\Omega))^d$, where $\tilde{a}_\theta(u, v) = (u, v) + \theta \Delta t v((u, v)) + \Delta t c(u^n, u, v)$ is a bilinear, continuous form on $(H_0^1(\Omega))^d$, which is coercive with respect to the norm $\|u\|$ (and hence to $\|u\|_1$); $c(u, v, w) = ((u \cdot \nabla)v, w)$ is a trilinear continuous form on $(H_0^1(\Omega))^d$ (if $d \leq 4$), which is skew-symmetric in v and w if $u \in V$; and $l_0 \in (H^{-1}(\Omega))^d$ is a known map. The coerciveness of $\tilde{a}_\theta$ results from the skew-symmetric character of the approximation of the convective term (which is a consequence of the assumed solenoidal character of u^n and the vanishing of u^n at the boundary) and the presence of the Laplacian term. The existence and uniqueness of $u^{n+1/2}$ is established by the Lax–Milgram theorem.

3.2. Second step

As far as the second step of the scheme is concerned, most known methods use the projection idea, which is based on a Hodge decomposition of a given vector field into a solenoidal field with zero normal component on the boundary and the gradient of some scalar function, or more specifically on the Ladyzenskaya theorem [27]. The incompatibility of the projection boundary conditions with those of the continuous problem and the need to impose unphysical boundary conditions on the pressure may result in the presence of a numerical boundary layer of size $O(v\Delta t)^{1/2}$ (see [9,11] for further discussions on this subject).

The method proposed herein includes a diffusion term in the incompressibility step, which allows for the imposition of the full boundary conditions for the velocity, while needing no boundary condition at all for the pressure. That is, given $u^{n+1/2}$ from Equation (4), one solves:

$$\frac{u^{n+1} - u^{n+1/2}}{\Delta t} - \theta v \nabla^2(u^{n+1} - u^{n+1/2}) + \nabla p^{n+1} = 0, \tag{6}$$

$$\operatorname{div} u^{n+1} = 0, \tag{7}$$

$$u^{n+1}|_\Gamma = 0. \tag{8}$$

Similar ideas to this scheme can be found in the so called θ-method of Glowinsky and others [28]. The θ-scheme is a three-step method developed from a two-step, fractional-step method. In the latter, the first step (or generalized Stokes problem) accounts for viscous effects together with incompressibility, but it also includes an explicit convective term and a force term; the second step (or regularized Burger's problem) also includes an implicit viscous term and a non-linear implicit approximation of convection, together with a pressure gradient and a force term, but not the incompressibility condition. The convergence of two fully discrete θ-schemes to a continuous solution was first proved by Fernández-Cara and Marín [29], where stability restrictions on the time step were also provided for those methods. Moreover, the inclusion of a viscous term in the incompressibility step of a fractional-step method can also be found in the method of [16], developed in a discrete setting, in the first and third steps of the method of [20], or in the example of a higher-order method in Section 7.5 of Reference [8], among others.

The weak form of Equations (6)–(8) consists of finding $u^{n+1} \in (H_0^1(\Omega))^d$ and $\phi^{n+1} = \Delta t p^{n+1} \in L_0^2(\Omega)$ such that:

$$a_\theta(u^{n+1}, v) + b(v, \phi^{n+1}) = l_1(v), \quad \forall v \in (H_0^1(\Omega))^d, \tag{9}$$

$$b(u^{n+1}, q) = 0, \quad \forall q \in L_0^2(\Omega), \tag{10}$$

where now $a_\theta(u, v) = (u, v) + \theta \Delta t v((u, v))$ is bilinear, symmetric, continuous form on $(H_0^1(\Omega))^d$, which is also coercive with respect to $\|u\|$; b is a bilinear continuous form defined on $(H_0^1(\Omega))^d \times L_0^2(\Omega)$ by $b(v, q) = -(\operatorname{div} v, q)$ and $l_1 \in (H^{-1}(\Omega))^d$ is known. The problem (9)–(10) is a mixed (or Stokes-type) problem, in which a_θ is coercive and b satisfies the inf–sup or Ladyzenskaya–Bubuŝka–Brezzi (LBB) condition [30]:

$$\inf_{q \in L_0^2(\Omega)} \left(\sup_{v \in (H_0^1(\Omega))^d} \frac{b(v, q)}{\|v\| \|q\|_{L_0^2(\Omega)}} \right) \geq \beta > 0,$$

so that the existence and uniqueness of u^{n+1} and p^{n+1} follows.

Remark 1

By adding (4) and (6) one gets:

$$\frac{u^{n+1} - u^n}{\Delta t} - \theta v \nabla^2 u^{n+1} - (1 - \theta) v \nabla^2 u^n + (u^n \cdot \nabla) u^{n+1/2} + \nabla p^{n+1} = \bar{f}^n, \tag{11}$$

where the implicit treatment of the viscous term in u^n and u^{n+1}, and not in the intermediate velocity $u^{n+1/2}$, can be observed. Moreover, it is clear from (11) that at least for the linear problem, p^{n+1} keeps its meaning as an end-of-step pressure. One advantage of using a split scheme like Equations (4)–(6) rather than a coupled (u, p) method, is the decoupling of the convective effects from incompressibility, which allows the use of suitable approximations for each term.

Remark 2

As in standard projection methods, a Poisson equation can be derived for the pressure to solve (6). In fact, taking the divergence of (6) yields:

$$\Delta t \nabla^2 p^{n+1} = (I - \theta \Delta t v \nabla^2) \operatorname{div}(u^{n+1/2}) \in H^{-1}(\Omega), \tag{12}$$

sufficient smoothness of the functions involved being assumed. But in order that Equations (12) and (6) imply (7), the incompressibility condition $\operatorname{div} u^{n+1} = 0$ must also be enforced on the boundary [31], as in the original method of [1]. Besides, boundary conditions for p^{n+1} cannot be directly derived, and p^{n+1} is subject to integral conditions [32]. Therefore, the original grad–div formulation (6)–(7) is adopted, which has the advantage of allowing discontinuous pressure approximations and requires no boundary conditions for this variable. One drawback of solving (6) and (7) is the need for the spatial approximation chosen to satisfy the discrete LBB condition [30], and that velocity and pressure unknowns have to be dealt with at the same time. However, it will be seen in Section 5 how they can still be decoupled.

Remark 3

A modified scheme with respect to (4) and (6) is considered next, which accounts for pressure correction [14]. A pressure update, rather than the pressure itself, is used in the incompressibility step, so that (4) becomes

$$\frac{u^{n+1/2} - u^n}{\Delta t} - \theta v \nabla^2 u^{n+1/2} - (1-\theta) v \nabla^2 u^n + (u^n \cdot \nabla) u^{n+1/2} + \nabla p^n = \bar{f}^n, \tag{13}$$

whereas (6) turns into

$$\frac{u^{n+1} - u^{n+1/2}}{\Delta t} - \theta v \nabla^2 (u^{n+1} - u^{n+1/2}) + \gamma \nabla(p^{n+1} - p^n) = 0, \tag{14}$$

where $0 < \gamma \leq 1$ is another free parameter. The addition of (13) and (14) shows the implicit treatment of the pressure term; this allows the use of the same approximation for this term as for the other terms by choosing $\gamma = \theta$, whereas (4)–(6) is necessarily a fully implicit scheme with respect to the pressure; in particular, the authors pretend to develop an extension of the present work to achieve second-order accuracy by taking $\theta = \gamma = 1/2$. Pressure correction can also be found in the methods of [26], with $\gamma = 1$, and [14], with $\gamma = 1/2$. The existence and uniqueness of solutions of (13) and (14) is established the same way as before.

4. CONVERGENCE OF THE METHOD

The fractional-step method introduced in the previous section is now shown to converge to a solution of the continuous problem, when the parameter θ is chosen equal to unity. The ideas used here follow a similar development to the proof of convergence of the original fractional-step method given by Temam [4]. After introducing some notation, a convergence theorem is given for some sequences of functions obtained from the intermediate and the end-of-step velocities of the fractional-step method. The proof of the theorem, as well as the preliminary results needed for it, is given in Appendix A.

Given $r \in [1, \infty)$, $T > 0$ and a Banach space W, the space $L^r(0, T; W)$ consists of functions defined on $(0, T)$ into W that are strongly r-integrable, i.e. such that

$$\|u\|_{L^r(0,T;W)} = \left(\int_0^T \|u(t)\|_W^r \, dt \right)^{1/r} < \infty.$$

It is also a Banach space with respect to the norm $\|u\|_{L^r(0,T;W)}$. The space of essentially bounded functions on $(0, T)$ into W is denoted by $L^\infty(0, T; W)$. When W is a Hilbert space with scalar product $(.\,,.)_W$, the space $L^2(0, T; W)$ is likewise with respect to:

$$(u, v) = \int_0^T (u(t), v(t))_W \, dt.$$

Let $T = N\Delta t$ and $k = \Delta t$, and consider the scheme consisting of (4) and (6) with $\theta = 1$. For this case, some approximating functions will be defined that will be piecewise equal to $u^{n+1/2}$, u^{n+1} or u^n. A linear interpolation between u^{n+1} and u^n is also introduced:

$$u_k^1 : [0, T] \rightarrow (L^2(\Omega))^d / u_k^1(t) = u^{n+1/2}, \quad nk \le t < (n+1)k,$$

$$u_k^2 : [0, T] \rightarrow (L^2(\Omega))^d / u_k^2(t) = u^{n+1}, \quad nk \le t < (n+1)k,$$

$$u_k^3 : [0, T] \rightarrow (L^2(\Omega))^d / u_k^3(t) = u^n, \quad nk \le t < (n+1)k.$$

$u_k : [0, T] \rightarrow (L^2(\Omega))^d / u_k$ is continuous, linear on t on each interval $[nk, (n+1)k]$ and $u_k(nk) = u^n$, for $n = 0, \ldots, N$.

The main result of this section is summarized in the following theorem:

Theorem 1
Let $d \le 4$, $f \in L^2 (0, T; H)$ and $u^0 \in V$. Then, there exists a subsequence k' of k and a solution u of (1) such that:

1. $u_{k'}^i$ and $u_{k'}$ converge to u in $L^2(\Omega \times (0, T))$ strongly, $i = 1, 2, 3$.
2. $u_{k'}^i$ and $u_{k'}$ converge to u in $L^\infty(0, T; (L^2(\Omega))^d)$ weak-star, $i = 1, 2, 3$.
3. $u_{k'}^i$ and $u_{k'}$ converge to u in $L^2(0, T; (H_0^1(\Omega))^d)$ weakly, $i = 1, 2, 3$.

For any other subsequence k'' such that these convergence results hold, u must be a solution of (1).

One also has:

Corollary 1
Let $d = 2$, $f \in L^2(0, T; H)$ and $u^0 \in V$. Then, the convergence given in Theorem 1 is of the sequence as a whole.

In summary, both the intermediate $u^{n+1/2}$ and the end-of-step velocities u^{n+1} are shown to converge weakly to $u(t_{n+1})$ in $(H_0^1(\Omega))^d$, through the functions u_k^1 and u_k^2 respectively. This is an improvement with respect to [4], where u^{n+1} only converges in $(L^2(\Omega))^d$. The introduction of pressure correction into the present method (as in (13) and (14)), which is the method that is actually implemented here) does not affect convergence. In [22], the authors prove this convergence to be of first-order in the time step for both the method with and without pressure correction, under stronger regularity assumptions on the data, the continuous solution and the domain.

5. SPACE DISCRETIZATION AND COMPUTATIONAL ASPECTS

Now consider space discretizations of the fractional-step, pressure correction method (13) and (14) with parameters $\theta = 1$ and $\gamma = 1$. Given two finite-dimensional spaces $V_h \subset (H_0^1(\Omega))^d$ and $Q_h \subset L_0^2(\Omega)$, the discrete equivalent to the weak form of problems (13) and (14) consists of finding $u_h^{n+1/2} \in V_h$, such that given $u_h^n \in V_h$ and $p_h^n \in Q_h$,

$$\frac{1}{\Delta t}(u_h^{n+1/2} - u_h^n, v_h) + v((u_h^{n+1/2}, v_h)) + c(u_h^n, u_h^{n+1/2}, v_h) + b(v_h, p_h^n) = (\bar{f}^n, v_h), \quad \forall v_h \in V_h$$

(15)

and $u_h^{n+1} \in V_h$ and $p_h^{n+1} \in Q_h$, such that

$$\frac{1}{\Delta t}(u_h^{n+1} - u_h^{n+1/2}, v_h) + v((u_h^{n+1} - u_h^{n+1/2}, v_h)) + b(p_h^{n+1} - p_h^n, v_h) = 0, \quad \forall v_h \in V_h,$$

(16)

$$b(u_h^{n+1}, q_h) = 0, \quad \forall q_h \in Q_h$$

respectively. The authors are mainly interested in the case when V_h and Q_h are defined through a discretization of Ω into finite elements. In particular, they consider two kinds of quadrilateral elements (in two dimensions): the bilinear velocity, constant pressure element ($Q_1 P_0$), which does not satisfy the discrete LBB condition, and the biquadratic velocity, linear pressure element ($Q_2 P_1$), which is *div-stable*.

The matrix form of Equations (15) and (16) is the following:

$$M\frac{U^{n+1/2} - U^n}{\Delta t} + K U^{n+1/2} + A(U^n)U^{n+1/2} + GP^n = \bar{F}^n,$$

(17)

$$M\frac{U^{n+1} - U^{n+1/2}}{\Delta t} + K(U^{n+1} - U^{n+1/2}) + G(P^{n+1} - P^n) = 0,$$

(18)

$$G^T U^{n+1} = 0,$$

(19)

where, here and in what follows, the following standard notation is used: U and P represent nodal velocity and elemental pressure vectors respectively, M is the mass matrix, K is the viscous-stiffness matrix, $A(U)$ is the advection matrix, G represents the discrete gradient operator, G^T being the discrete divergence, and $\bar{F}^n$ is a forcing term due to the term $\bar{f}^n$ and to non-homogeneous Dirichlet boundary conditions (see [24] for precise definitions of these matrices).

The numerical solution of these equations presents some problems. On the one hand, the system matrix for the intermediate velocity equation (17) has to be computed and factorized once every time step, due to the implicit approximation of the convective term; moreover, this matrix is not symmetric since the convective term is skew-symmetric. On the other hand, the coupled system (18)–(19) has the structure of a mixed problem. Equation (18) can be rewritten as:

$$B(U^{n+1} - U^{n+1/2}) + \Delta t G(P^{n+1} - P^n) = 0,$$

(20)

where $B = M + \Delta t K$. One can then isolate U^{n+1} from (20) (the matrix B being positive definite, and thus invertible) and substitute it into (19), thus segregating the computation of the pressure from that of the velocity; this yields:

$$(G^T B^{-1} G)(P^{n+1} - P^n) = \frac{1}{\Delta t} G^T U^{n+1/2}.$$

(21)

But the computation of the system matrix for this pressure equation requires the inversion of a full matrix B, which is prohibitive in most cases. The authors present an alternative way to solve (17)–(19), which bypasses the problem of inverting the matrix B at the cost of introducing a few iterations per time step.

Following similar ideas of the predictor–multicorrector algorithm to be studied in the next section, the authors consider an iterative solution of the discrete Equations (17)–(19). Each iteration consists of the solution of two diagonal systems and another system with a symmetric, positive (semi-) definite matrix. The latter matrix needs to be computed and factorized only once at the beginning of the calculation; the computational cost of each iteration is then only due to the formation of three residual vectors, the solution of two diagonal systems and a backward and forward substitution. Since only a few iterations of the proposed scheme are needed for convergence in each time step (see the numerical examples of Section 7), this iterative procedure is more efficient than solving the original Equations (17)–(19). Recall that these equations require the computation and factorization of a non-symmetric matrix for the intermediate velocity system and the solution of a Stokes-like problem in each time step.

Given the nth step values U^n and P^n of velocities and pressures respectively, the iterative procedure starts with the initializations $U_0^{n+1/2} = U^n$, $U_0^{n+1} = U^n$ and $P_0^{n+1} = P^n$ for the values at time t_{n+1}. Then, if $U_i^{n+1/2}$ and U_i^{n+1} are the ith iteration approximations to $U^{n+1/2}$ and U^{n+1} respectively, consider the scheme:

$$M \frac{U_{i+1}^{n+1/2} - U^n}{\Delta t} + K U_i^{n+1/2} + A(U^n) U_i^{n+1/2} + G P^n = F^n, \tag{22}$$

$$M \frac{U_{i+1}^{n+1/2} - U_{i+1}^{n+1/2}}{\Delta t} + K(U_i^{n+1} - U_i^{n+1/2}) + G(P_{i+1}^{n+1} - P^n) = 0, \tag{23}$$

$$G^T U_{i+1}^{n+1} = 0. \tag{24}$$

At convergence, i.e. when $U_{i+1}^{n+1/2} = U_i^{n+1/2}$, $U_{i+1}^{n+1} + U_i^{n+1}$ and $P_{i+1}^{n+1} = P_i^{n+1}$, these values satisfy (17)–(19). The implemented stopping criterion is:

$$\max \left(\frac{|U_{i+1}^{n+1} - U_i^{n+1}|_2}{|U_{i+1}^{n+1}|_2}, \frac{|U_{i+1}^{n+1/2} - U_i^{n+1/2}|_2}{|U_{i+1}^{n+1/2}|_2}, \frac{|P_{i+1}^{n+1} - P_i^{n+1}|_2}{|P_{i+1}^{n+1}|_2} \right) \leq \epsilon,$$

where $|X|_2$ is the Euclidean norm of a vector X.

U_{i+1}^{n+1} can also be isolated from (23) and substituted into (24), so as to segregate the computation of the pressure from that of the velocity. By doing this, one obtains

$$(G^T M^{-1} G)(P_{i+1}^{n+1} - P^n) = \frac{1}{\Delta t} G^T(U_{i+1}^{n+1/2} - \Delta t M^{-1} K(U_i^{n+1} - U_i^{n+1/2})). \tag{25}$$

To make the scheme computationally efficient, matrix M is approximated by its lumped diagonal M^L everywhere except for the evaluation of the residuals. The computation of the system matrix for (25) then becomes feasible, since the inversion it involves is then trivial.

The actual implementation of the scheme, however, is somewhat different. It is given in terms of nodal accelerations $\mathscr{A}$ and time derivatives of elemental pressures, $\dot{P}$. Calling $\mathscr{A}_{i+1}^{n+1/2} = (U_{i+1}^{n+1/2} - U^n)/\Delta t$, $\mathscr{A}_{i+1}^{n+1} = (U_{i+1}^{n+1} - U_{n+1}^{n+1/2})/\Delta t$ and $\dot{P}_{i+1}^{n+1} = (P_{i+1}^{n+1} - P^n)/\Delta t$, Equations (22), (25) and (23) can be written, with the approximation of M by M^L, as

$$M^L \mathscr{A}_{i+1}^{n+1/2} = R_1,$$

$$(\Delta t)^2 (G^T (M^L)^{-1} G) \dot{P}_{i+1}^{n+1} = R_p,$$

$$M^{\mathrm{L}}\mathscr{A}_{i+1}^{n+1} = R_2,$$

where:

$$R_1 = F^n - KU_i^{n+1/2} - A(U^n)U_i^{n+1/2} - GP^n,$$

$$U_{i+1}^{n+1/2} = U^n + \Delta t \mathscr{A}_{i+1}^{n+1},$$

$$R_p = G^T(U_{i+1}^{n+1/2} - \Delta t^2(M^{\mathrm{L}})^{-1}K\mathscr{A}_i^{n+1}),$$

$$R_2 = -\Delta t(G\dot{P}_{i+1}^{n+1} + K\mathscr{A}_i^{n+1}).$$

6. THE PREDICTOR–MULTICORRECTOR ALGORITHM

The predictor–multicorrector algorithm of [23] can be understood in the context of fractional-step methods. To see this, the incompressible Navier–Stokes equations (1) will be first approximated by an implicit method of the form:

$$\frac{u^{n+1} - u^n}{\Delta t} - \alpha a^{n+1} - (1-\alpha)a^n = 0, \tag{26}$$

$$\mathrm{div}(u^{n+1}) = 0, \tag{27}$$

$$u^{n+1}|_\Gamma = 0, \tag{28}$$

where $a^m = f^m - \nabla p^m - (u^m \cdot \nabla)u^m + \nu\nabla^2 u^m$, $f^m = f(m\Delta t)$ and $0 < \alpha \le 1$. An iterative scheme is introduced for the solution of the non-linear, coupled problems (26)–(28). It begins with some predictions u_0^{n+1} and p_0^{n+1} for u^{n+1} and p^{n+1} respectively. Then, each iteration is split into two steps. The first one accounts for the momentum equation but not for the incompressibility condition, which is dealt with in the second step, in a similar way to the scheme of Section 3. The convective term is made explicit for simplicity, and pressure correction is used (see Remark 3); this way, given the ith iteration approximations u_i^{n+1} and p_i^{n+1} to u^{n+1} and p^{n+1}, the first step consists of finding an *intermediate iteration* velocity $u_{i+1/2}^{n+1}$ such that:

$$\frac{u_{i+1/2}^{n+1} - u^n}{\Delta t} - \alpha\nu\nabla^2 u_{i+1/2}^{n+1} = \alpha f^{n+1} + (1-\alpha)a^n - \alpha(u_i^{n+1} \cdot \nabla)u_i^{n+1} - \alpha\nabla p_i^{n+1}, \tag{29}$$

$$u_{i+1/2}^{n+1}|_\Gamma = 0. \tag{30}$$

(The notation $u_{i+1/2}^{n+1}$ has been chosen deliberately to emphasise that the solution of (29) is an intermediate iteration approximation of the velocity at time t_{n+1}.) In the second step of each iteration, a pressure increment is used to enforce incompressibility, in a similar way to the pressure correction method of Remark 3 in Section 3. Thus, one looks for an *end-of-iteration* velocity u_{i+1}^{n+1} and pressure p_{i+1}^{n+1} such that:

$$\frac{u_{i+1}^{n+1} - u_{i+1/2}^{n+1}}{\Delta t} - \alpha\nu\nabla^2(u_{i+1}^{n+1} - u_{i+1/2}^{n+1}) + \alpha\nabla(p_{i+1}^{n+1} - p_i^{n+1}) = 0, \tag{31}$$

$$\mathrm{div}\, u_{i+1}^{n+1} = 0, \tag{32}$$

$$u_{i+1}^{n+1}|_\Gamma = 0. \tag{33}$$

The iterative scheme (29)–(31)–(32) is a generalized version of the predictor–multicorrector algorithm of [23]. In the fully implicit case, $\alpha = 1$, the scheme (13)–(14) of Section 3, with $\theta = \gamma = 1$, is also equivalent to this algorithm if only one iteration per time step is performed,

since then $u_0^{n+1} = u^n$ and $p_0^{n+1} = p^n$ [33]; however, this algorithm employs an explicit treatment of the convective term in that case. The correspondence between the different variables is then: $u_{1/2}^{n+1} = u^{n+1/2}$, $u_1^{n+1} = u^{n+1}$ and $p_1^{n+1} = p^{n+1}$.

The semi-discrete scheme of (29)–(31)–(32) is further discretized in space by a Galerkin finite element interpolation of mixed type. The same two element pair combinations are considered again, i.e. the bilinear velocity, constant pressure element ($Q_1 P_0$) and the biquadratic velocity, linear pressure element ($Q_2 P_1$). The finite element approximation of (29), (31) and (32) yields the following systems of linear equations:

$$B(U_{i+1/2}^{n+1}) = F_1, \tag{34}$$

$$B(U_{i+1}^{n+1}) + \alpha G(P_{i+1}^{n+1}) = F_2, \tag{35}$$

$$G^T(U_{i+1}^{n+1}) = 0, \tag{36}$$

where now $B = M + \alpha \Delta t K$, $F_1 = MU^n + \Delta t(F^{n+1} + (1 - \alpha)M \mathscr{A}^n - \alpha A(U_i^{n+1})U_i^{n+1} - \alpha GP_i^{n+1})$ and $F_2 = BU_{i+1/2}^{n+1} + \alpha GP_i^{n+1}$. By isolating U_{i+1}^{n+1} from (35) and substituting it into (36), one gets:

$$(G^T B^{-1} G)(P_{i+1}^{n+1}) = F_3, \tag{37}$$

where

$$F_3 = \frac{1}{\Delta t \alpha} G^T U_{1+1/2}^n + (G^T B^{-1} G) P_i^{n+1}$$

and the equation system (37) and (35) is equivalent to (35) and (36). Upon implementation of the predictor–multicorrector algorithm, matrix B is usually approximated by M in all its appearances, the difference between the two being of order Δt. Moreover, the matrix M is further simplified by a *lumping* process, resulting in a diagonal matrix M^L. These simplifications have a double theoretical implication: on the one hand, the approximation of B by M in (34) leads to an explicit treatment of diffusion in each iteration (although not in each time step, if the algorithm is iterated at least twice per step); on the other hand, the approximation of B by M in (35) and (37) implies that the algorithm actually used admits an interpretation within the context of fractional-step methods relative to the standard projection method, i.e. without a viscous term in the incompressibility phase. A single iteration of this simplified predictor–multicorrector algorithm is actually equivalent to the standard projection method. Then a classical question arises: which boundary conditions are to be imposed in the incompressibility phase: the full Dirichlet condition or only the normal component of it?

If two or more iterations of this scheme are performed, given the implicit character of the approximation of the viscous and convective terms, no Δt limitations are expected for the stability of the algorithm in a wide range of Reynolds number. However, the iterative nature of the scheme and the simplifications introduced in it (such as the explicit treatment of the convective term) impose restrictions on Δt for the stability (and convergence) of the iterative process.

7. NUMERICAL RESULTS

The authors present the results obtained with the fractional-step pressure correction method with parameters $\theta = \gamma = 1$ on three test problems. The first one is a test case introduced by van Kan [14], intended to study numerically the order of approximation of the scheme in the time

step; the authors also solved this case with the predictor–multicorrector algorithm; the second one is the classical problem of steady flow over a backward facing step, and the third one is the problem of flow around a cylinder.

7.1. Numerical accuracy study

As a numerical check for the accuracy properties of the method, a test case introduced by van Kan [14] is considered. It consists of the Navier–Stokes flow on a unit square cavity in which an inflow velocity profile is prescribed at the top wall defined by $u((x, 1), t) = (0, -\sin(\pi(x^3 - 3x^2 + 3x))\exp(1 - 1/t))$ for $0 \leq x \leq 1$ and $t > 0$, the bottom and left walls are solid walls and natural boundary conditions are enforced on the right, outlet wall. As in [14], a Reynolds number of 10 was selected, and the fluid was at rest at the start. A uniform mesh consisting of 6×6 elements was used for the Q_1P_0 case; in order to compare the results from

Table I. Van Kan's flow, fractional-step method, Q_1P_0 element

Δt	$\kappa_1(\Delta t)$	$\kappa_2(\Delta t)$	$\kappa_p(\Delta t)$
1/60	2.1	3.5	2.3
1/64	2.0	3.4	2.4
1/80	2.0	3.0	2.2
1/85	2.0	2.9	2.1

Table II. Van Kan's flow, fractional-step method, Q_2P_0 element

Δt	$\kappa_1(\Delta t)$	$\kappa_2(\Delta t)$	$\kappa_p(\Delta t)$
1/75	2.2	3.5	2.5
1/80	2.1	3.3	2.5
1/85	2.1	3.1	2.4

Table III. Van Kan's flow, predictor–multicorrector algorithm, Q_1P_0 element, $\alpha = 1$, one iteration per step (classical projection method)

Δt	$\kappa_1(\Delta t)$	$\kappa_2(\Delta t)$	$\kappa_p(\Delta t)$
1/16	2.04	2.02	2.03
1/32	2.02	2.01	2.02
1/64	2.01	2.01	2.01
1/128	1.99	1.99	2.00

Table IV. Van Kan's flow, predictor–multicorrector algorithm, Q_1P_0 element, $\alpha = 1/2$, iterating to convergence

Δt	$\kappa_1(\Delta t)$	$\kappa_2(\Delta t)$
1/7	4.06	4.08
1/8	4.04	4.04
1/10	4.03	4.01
1/12	3.75	3.99
1/14	4.00	3.79

Table V. Van Kan's flow, predictor–multicorrector algorithm, Q_2P_1 element, $\alpha = 1$, one iteration per step (classical projection method)

Δt	$\kappa_1(\Delta t)$	$\kappa_2(\Delta t)$	$\kappa_p(\Delta t)$
1/16	2.24	2.27	2.04
1/32	2.01	1.99	2.02
1/64	2.00	1.99	2.01
1/128	1.97	1.99	2.01

Table VI. Van Kan's flow, predictor–multicorrector algorithm, Q_2P_1 element, $\alpha = 1/2$, iterating to convergence

Δt	$\kappa_1(\Delta t)$	$\kappa_2(\Delta t)$
1/16	3.83	4.15
1/20	3.96	4.04
1/24	3.86	3.92

both interpolations, the same mesh points were used to define a 3×3 mesh for the Q_2P_1 element.

Let $\kappa_i(\Delta t)$ denote the quotient:

$$\kappa_i(\Delta t) = \frac{|U_i(\Delta t) - U_i(\tfrac{1}{2}\Delta t)|_2}{|U_i(\tfrac{1}{2}\Delta t) - U_i(\tfrac{1}{4}\Delta t)|_2},$$

where U_i ($i = 1, 2$) contains the ith component of the nodal velocities obtained at $t = 1$ with the indicated time step. Similarly, $\kappa_p(\Delta t)$ denotes the same quotient for the elemental pressure (and eventually, pressure spatial derivative) values.

Tables I and II show the most accurate results obtained with the fractional-step, pressure correction method with parameters $\theta = \gamma = 1$ for the two different space interpolations. The value of the tolerance was fixed to $\epsilon = 10^{-4}$; convergence of the iterative scheme was reached in 10 or 11 iterations, for the largest time steps, to 3 or 4 for the smallest. It can be observed that the scheme is, at least asymptotically, first-order-accurate in the time step both in velocities and in pressures.

In Tables III–VI, the results obtained for this problem with the predictor–multicorrector algorithm for the two different finite element interpolations are shown. In the backward Euler case ($\alpha = 1$), first-order accuracy is achieved with only one correction per time step, for both 4-noded and 9-noded elements. This confirms that the approximation of the matrix B by M^L introduces an error that is of first-order in the time step. It can be seen that in all cases, the pressure approximation is also first-order-accurate. First-order accuracy was also reached in other cases: performing two iterations every time step and iterating to convergence in each time step (which took an average of ten iterations per time step to reduce the initial residuals by seven orders of magnitude).

The Crank–Nicholson case ($\alpha = 1/2$) is a second-order method. Nevertheless, iterating to convergence is compulsory in this case to maintain the second-order accuracy of the scheme. If a fixed number of two iterations per time step is chosen, second-order accuracy is lost.

7.2. Backward-facing step

The well-known problem of the flow over a backward facing step is presented next. This problem was extensively studied by Armaly *et al.* [34], both experimentally and numerically; other numerical results can be found in [15,35,36]. Here a geometry similar to that of [34] is considered, i.e. an inflow channel of length 2 and height 1, an expansion ratio of 1:1.90 and a total channel length of 40. A Poiseuille parabolic profile is prescribed at the inflow, with a maximum velocity of 1; the top and bottom sides are solid walls, and natural boundary conditions are enforced at the outlet. The mesh used for this problem, which is finer near the step, can be seen in Figure 1, where the y-axis has been magnified three times; it consists of 1305 mesh points, which were used to define both the Q_1P_0 and the Q_2P_1 elements. There are 1220 and 305 of such elements respectively.
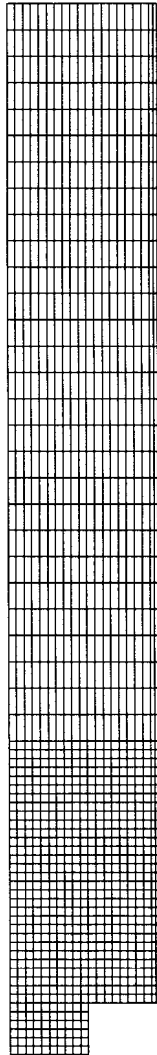
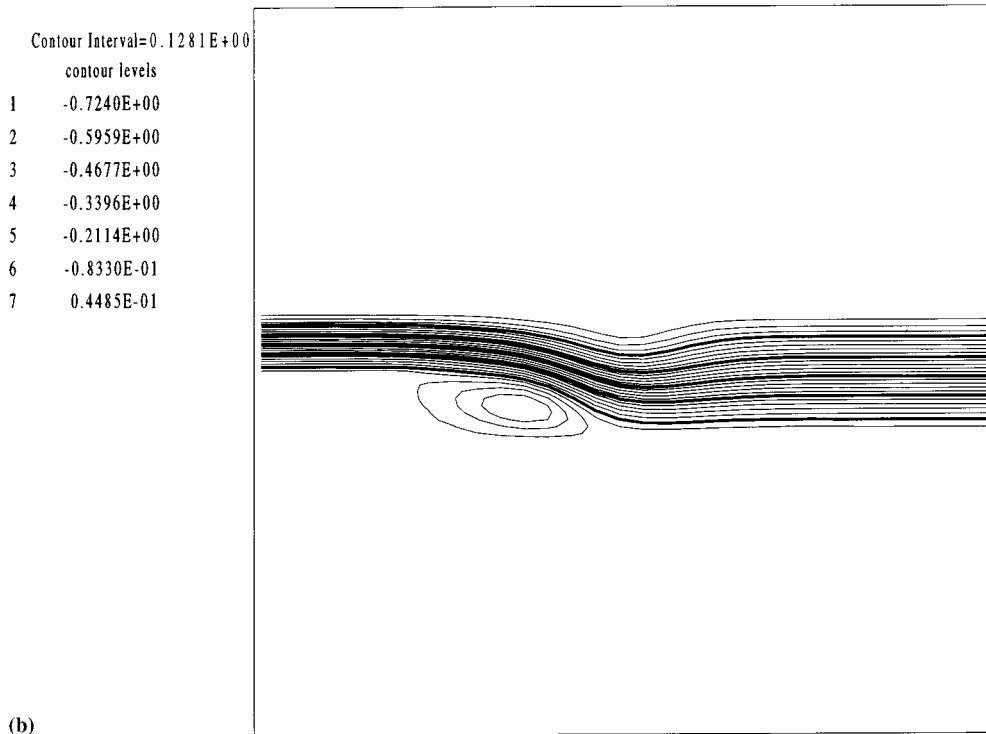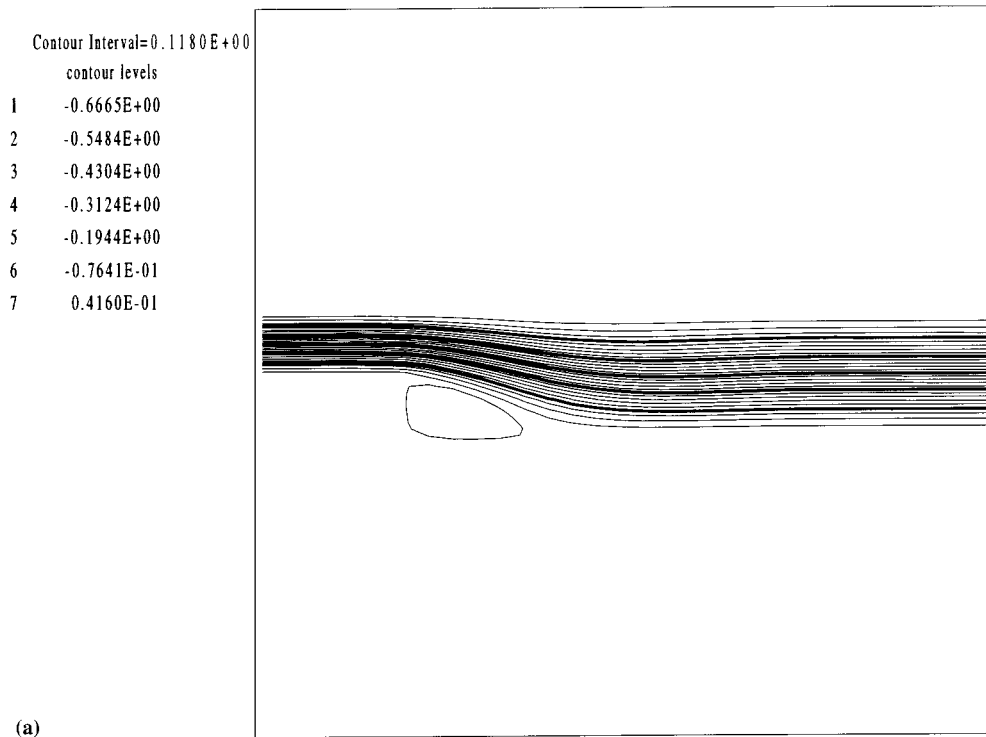Figure 1. Backward-facing step, mesh.

Contour Interval=0.1180E+00

contour levels

1	-0.6665E+00
2	-0.5484E+00
3	-0.4304E+00
4	-0.3124E+00
5	-0.1944E+00
6	-0.7641E-01
7	0.4160E-01

(a)

Contour Interval=0.1281E+00

contour levels

1	-0.7240E+00
2	-0.5959E+00
3	-0.4677E+00
4	-0.3396E+00
5	-0.2114E+00
6	-0.8330E-01
7	0.4485E-01

(b)

Figure 2. Backward-facing step, Q_1P_0 element, streamlines: (a) $Re = 60$; (b) $Re = 200$; (c) $Re = 400$.

Contour Interval=0.5823E-01

contour levels

1	-0.7723E+00
2	-0.7140E+00
3	-0.6558E+00
4	-0.5976E+00
5	-0.5393E+00
6	-0.4811E+00
7	-0.4229E+00
8	-0.3647E+00
9	-0.3064E+00
10	-0.2482E+00
11	-0.1900E+00
12	-0.1317E+00
13	-0.7351E-01
14	-0.1528E-01
15	0.4295E-01

(c)
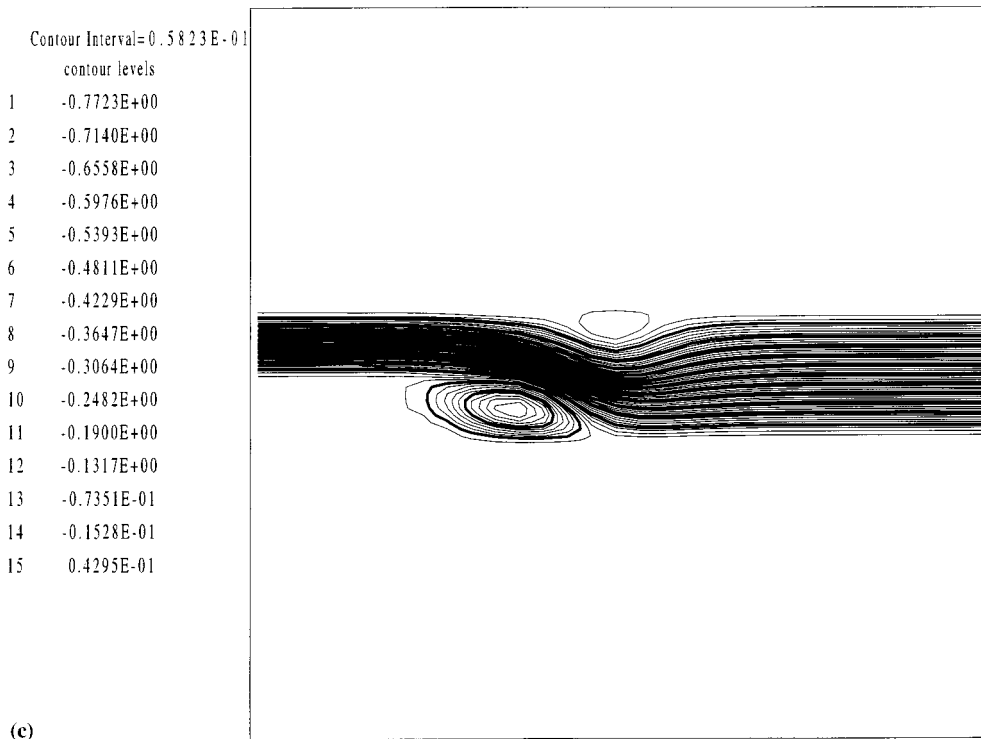
Figure 2 (*Continued*)

This problem is solved with the present fractional-step method for three different values of the Reynolds number: 40, 200 and 400. The Reynolds number is characterized by the average inflow velocity (which is 4/3 for the data considered here), and the inflow channel height. For this range of Reynolds numbers, the flow is virtually two-dimensional (see the experimental results in [34]), so that planar numerical models are meaningful. The results are obtained with a time step $\Delta t = 0.01$ and following the scheme (22)–(24) up to convergence (with a tolerance of $\epsilon = 10^{-3}$) at each time step (only three or four iterations are needed during the initial steps decreasing to only one in the last steps). Steady state is considered when the accelerations are in the order of 10^{-5}.

Figures 2 and 3 present the results obtained for the different Reynolds numbers for the $Q_1 P_0$ element and for the $Q_2 P_1$ respectively, in the form of steady streamlines, where the x-axis is limited to the range [0, 10]. It can be clearly observed in these figures how the reattachment length of the main vortex increases with increasing Reynolds numbers, a characteristic of the flow that is well-known for this problem, since the work is within the laminar Reynolds number range [34]. Moreover, the appearance of a secondary separation bubble on the no-step wall at $Re = 400$ can also be observed, which is in good agreement with the experimental results of [34].

7.3. Flow past a circular cylinder

Finally, the challenging problem of the flow past a circular cylinder is considered. It has attracted the attention of several authors, [23,37–42] for instance. This has become a compulsory benchmark test for transient algorithms for Navier–Stokes equations.
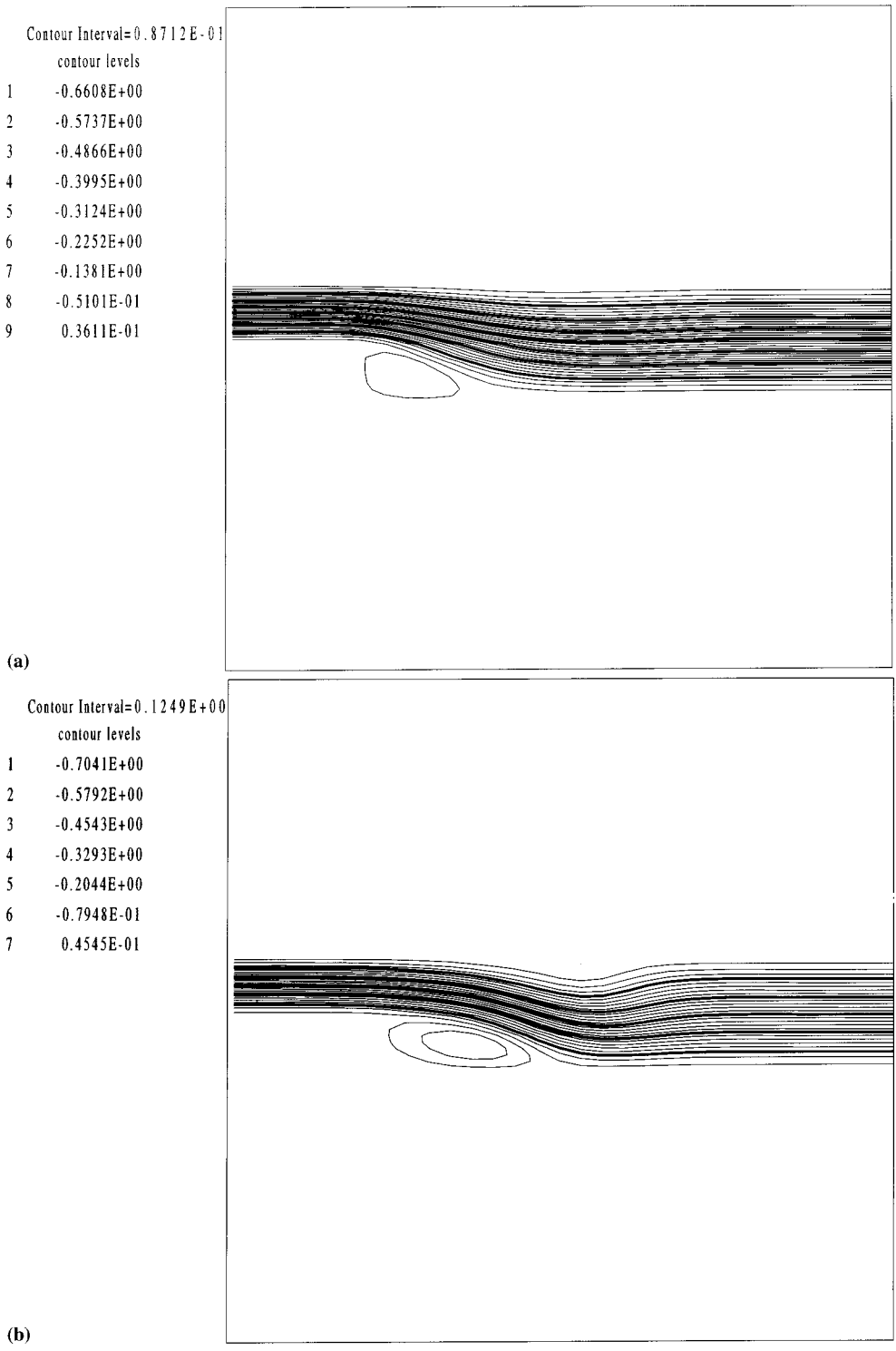
Contour Interval=0.8712E-01
contour levels
1   -0.6608E+00
2   -0.5737E+00
3   -0.4866E+00
4   -0.3995E+00
5   -0.3124E+00
6   -0.2252E+00
7   -0.1381E+00
8   -0.5101E-01
9   0.3611E-01

(a)

Contour Interval=0.1249E+00
contour levels
1   -0.7041E+00
2   -0.5792E+00
3   -0.4543E+00
4   -0.3293E+00
5   -0.2044E+00
6   -0.7948E-01
7   0.4545E-01

(b)

Figure 3. Backward-facing step, Q_2P_1 element, streamlines: (a) $Re = 60$; (b) $Re = 200$; (c) $Re = 400$.

Contour Interval=0.4889E-01

contour levels

1	-0.7430E+00
2	-0.6941E+00
3	-0.6452E+00
4	-0.5963E+00
5	-0.5474E+00
6	-0.4986E+00
7	-0.4497E+00
8	-0.4008E+00
9	-0.3519E+00
10	-0.3030E+00
11	-0.2541E+00
12	-0.2052E+00
13	-0.1563E+00
14	-0.1074E+00
15	-0.5855E-01
16	-0.9665E-02
17	0.3922E-01

(c)
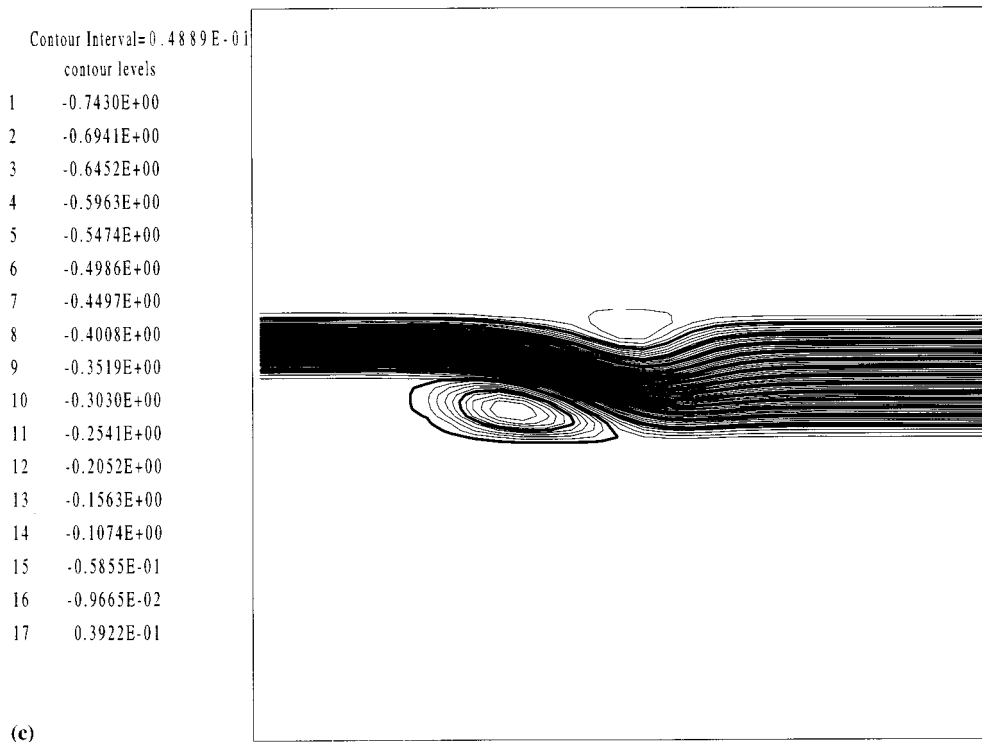
Figure 3 (*Continued*)

It is well-known that for low values of the Reynolds number, the solution is steady and symmetric about a line parallel to the free-stream flow through a cylinder diameter; a pair of symmetrical eddies develops downstream of the cylinder. But beyond a critical value of *Re* (which is > 40), the steady solution becomes unstable and a periodic solution develops, so that vortex shedding sets in; vortices begin to generate periodically and alternately from each side of the cylinder, and are 'transported' by the flow away from it. This scenario is known in the literature as a von Karman vortex street.

A cylinder of unit diameter and a computational domain consisting of the rectangle $[0, 21] \times [0, 9]$ are considered, the center of the cylinder being situated at the point $(4.5, 4.5)$. These data, however, may not be sufficient to prevent any effect of the introduction of artificial boundaries on the computed solution, as was recently studied in [37], which discussed the influence of the location of the lateral boundaries on the computed flow field; it can still be seen how this may affect the computations. A unit free-stream horizontal velocity was prescribed on the left boundary, a vertical zero velocity on the upper and lower boundaries and natural conditions are enforced everywhere else. The mesh used in this case can be seen in Figure 4, which consists of 3000 nodes and 2880 of the $Q_1 P_0$ elements.

First, the problem for $Re = 40$ is solved. The scheme (22)–(24) was iterated to convergence in each time step with a tolerance of $\epsilon = 10^{-2}$, which took an average of two iterations. After 1000 steps of size $\Delta t = 0.005$, the steady, symmetric solution is reached, with accelerations in the order of 10^{-4}. This steady situation can be seen in Figures 5–7, where the streamlines, the stationary streamlines and the nodal pressure contours obtained from the elemental pressures after a least-squares interpolation process are shown respectively. Symmetry is very accurately achieved.
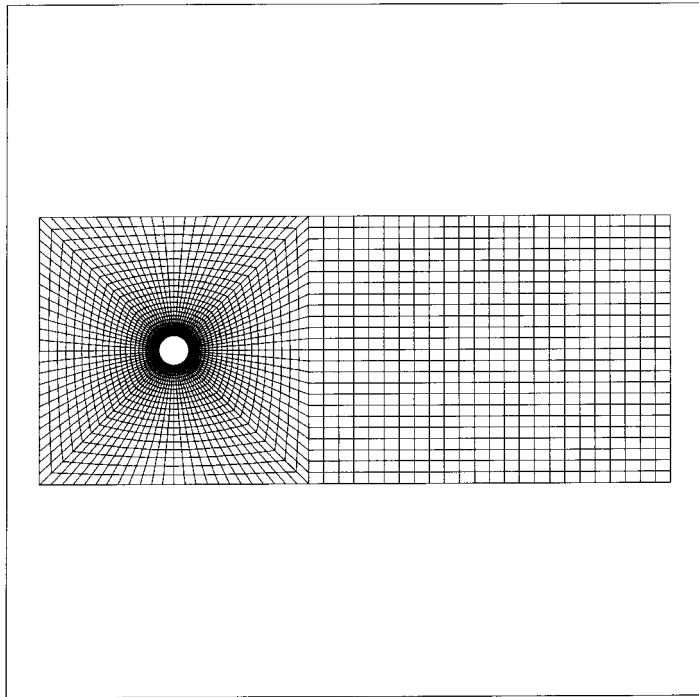
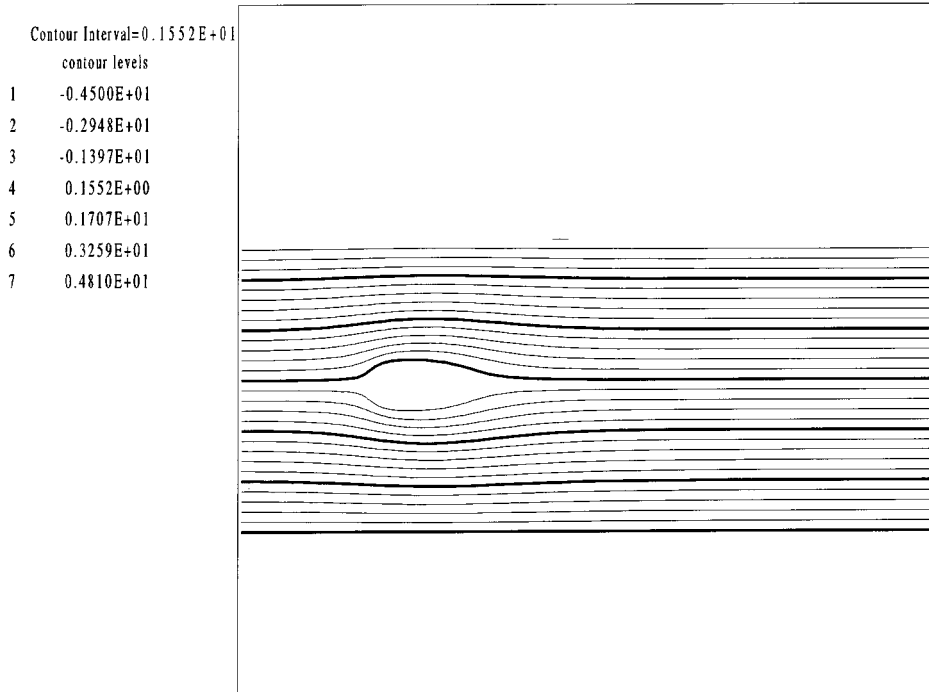Figure 4. Flow past a cylinder, mesh.
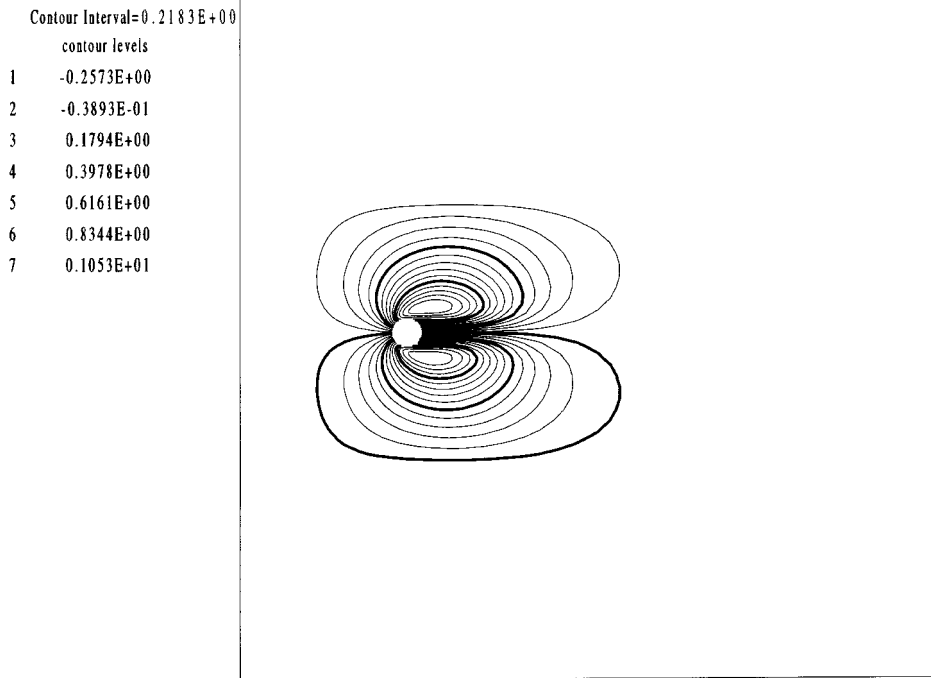

Figure 5. Flow past a cylinder, $Re = 40$, streamlines.

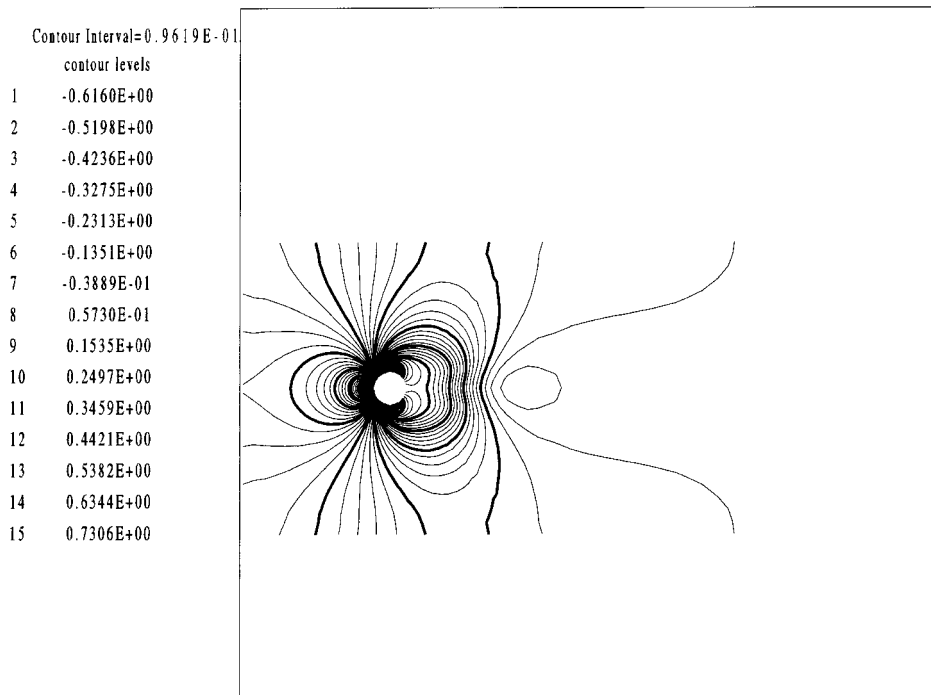Figure 6. Flow past a cylinder, $Re = 40$, stationary streamlines.

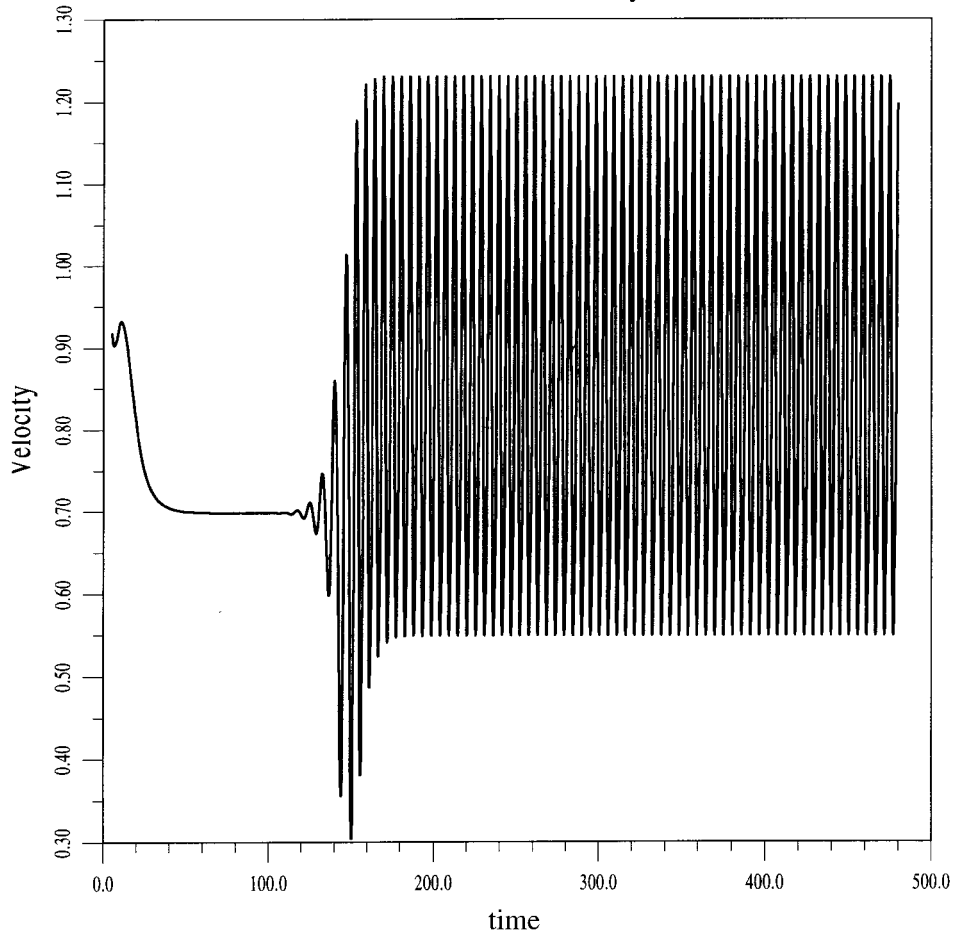Figure 7. Flow past a cylinder, $Re = 40$, nodal pressure contours.

Nodal Velocity

Figure 8. Flow past a cylinder, $Re = 100$, nodal velocity history.

Then the value of the Reynolds number was raised to 100, which is the one commonly used for this problem. The computation was started from the steady solution obtained for $Re = 40$, and performed 19 000 steps of size $\Delta t = 0.025$; in each of them, one or two iterations were enough to reach convergence at the same value of the tolerance as before. It was found that the solution started oscillating freely at a time near $t = 110$; the final periodicity of the solution was reached by $t = 170$. Figure 8 shows the history of the horizontal velocity at a node situated at the point (9.0, 5.25), i.e. downstream of the cylinder and slightly higher. The qualitative change in the solution regime can be clearly observed. In this case, no artificial trick was needed to start up the periodic solution.

The streamlines obtained at the end of the computation ($t = 475$) are shown in Figure 9. Figure 10 plots the stationary streamlines; the wakes behind the cylinder can be clearly seen there. Finally, the pressure contours are shown in Figure 11. All these results compare very well with other published solutions [23,38,40,42].
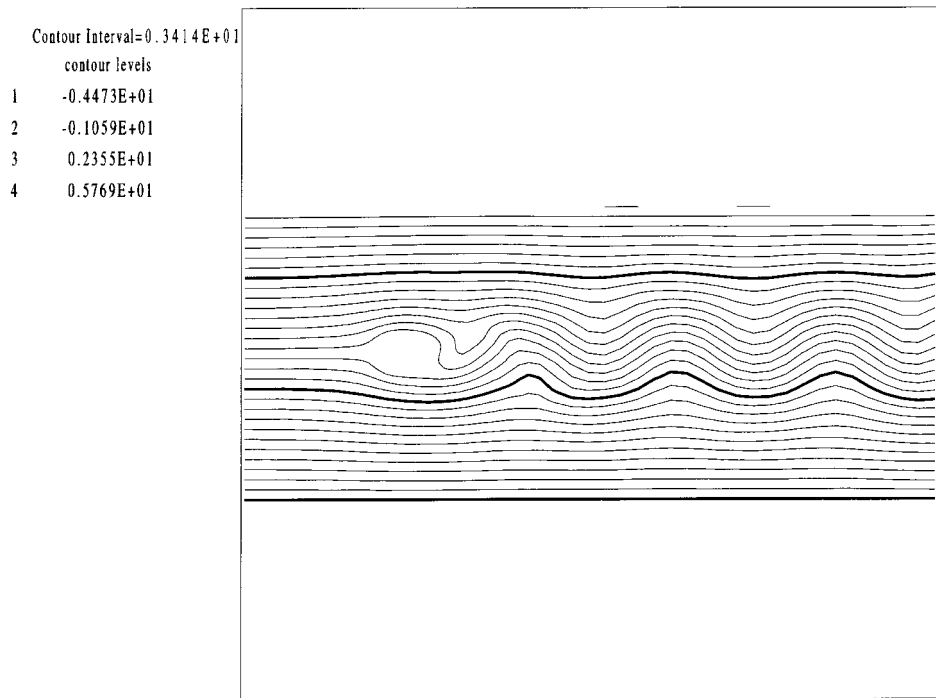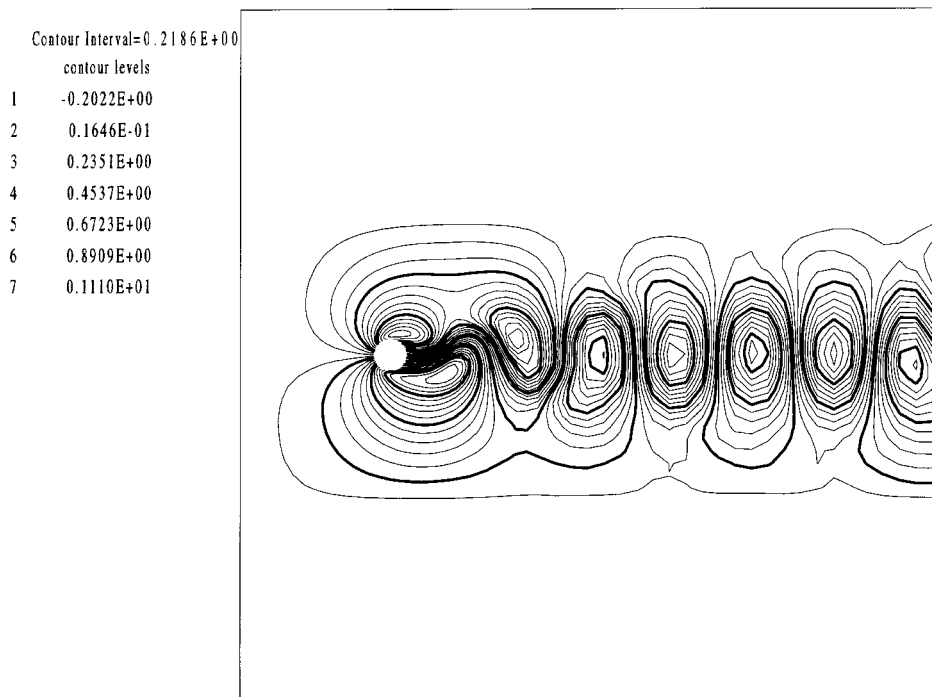
Contour Interval=0.3414E+01

contour levels

1   -0.4473E+01

2   -0.1059E+01

3   0.2355E+01

4   0.5769E+01

Figure 9. Flow past a cylinder, $Re = 100$, streamlines.

Contour Interval=0.2186E+00

contour levels

1   -0.2022E+00

2   0.1646E-01

3   0.2351E+00

4   0.4537E+00

5   0.6723E+00

6   0.8909E+00

7   0.1110E+01

Figure 10. Flow past a cylinder, $Re = 100$, stationary streamlines.
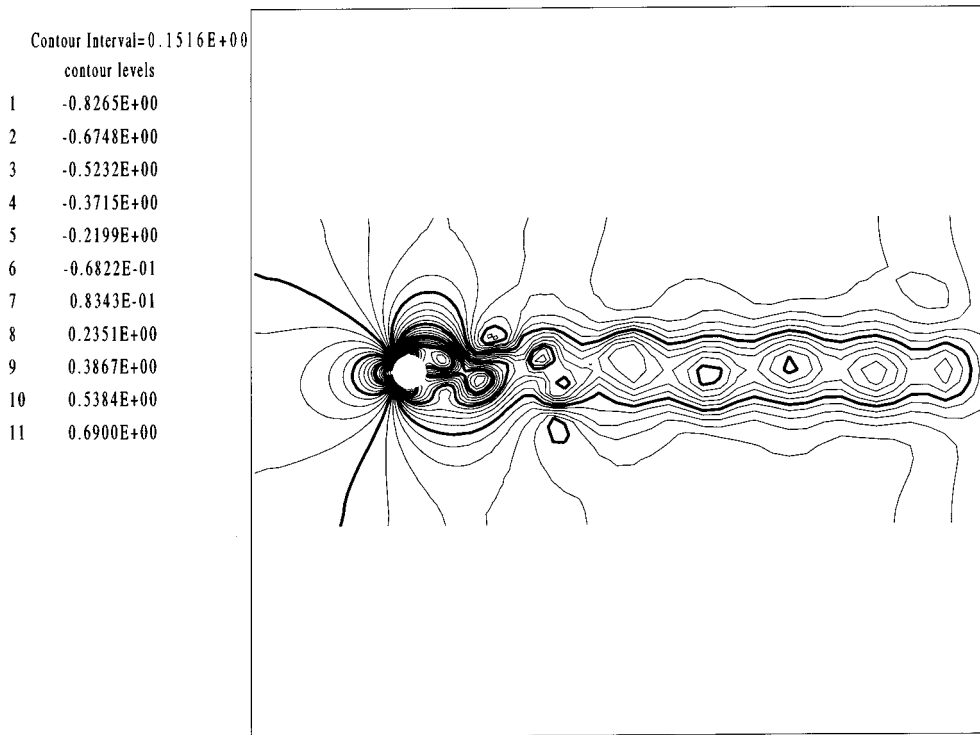
Figure 11. Flow past a cylinder, $Re = 100$, nodal pressure contours.

Some flow features are generally used to compare quantitatively the solutions obtained for this problem. The Strouhal number or adimensional frequency of the solution is one of the most studied quantities; it is defined as $St = D/u_0\tau$, where D is the cylinder diameter, u_0 is the free-stream velocity (in this case, both equal to 1) and τ is the shedding period of the solution. A Fourier analysis of the nodal velocity signal was performed within the time range [175, 475] (i.e. for most of the developed periodic solution) in order to find the dominant frequency of the solution. In Figure 12, the Fourier spectrum obtained is shown, from which a Strouhal number of $St = 0.18667$ was found (smaller peaks can also be seen at twice and three times that frequency), or equivalently, a period of 5.3571. This period is somewhat smaller than the one generally admitted for this value of Reynolds number, which is 6, i.e. a Strouhal number of $St = 0.16667$ [23]. This discrepancy is attributed to the fact that a standard Galerkin finite element interpolation was used, which is less dissipative than stabilized formulations of the SUPG or GLS type usually employed for this problem. However, discrepancies in the value of the Strouhal number depending on the formulation employed were also found by other authors [40,42]. Moreover, the location of the lateral boundaries in the current computational domain may not be far enough from the cylinder to avoid any influence on the solution of the artificial boundary conditions introduced by the formulation; in fact, it was obtained in [37] that at least 12 cylinder diameters on each side of the cylinder are needed to avoid that influence, otherwise larger Strouhal numbers were obtained. This may be another cause of the increase of the computed Strouhal number.

8. CONCLUSIONS

In this paper a fractional step method for the approximation of the incompressible Navier–Stokes equations in primitive variables has been studied, which depends on a free parameter $\theta \in (0, 1]$. For $\theta = 1$, both the intermediate and the end-of-step velocities have been shown to converge to an exact solution in the space $(H_0^1(\Omega))^d$. By introducing a viscous term in the second step of the scheme, full boundary conditions are imposed on the velocity in all steps. Thus, this method does not introduce the numerical boundary layer present in some other fractional-step methods. One drawback of this formulation is the need for the space interpolations of velocity and pressure to satisfy the compatibility conditions met when solving the Stokes problem in primitive variables.

Moreover, this method has been related to an existing predictor–multicorrector algorithm. A new derivation of the algorithm, in a more general context than the classical one, has been given, showing in what sense it can be considered as a fractional-step iterative method. Two
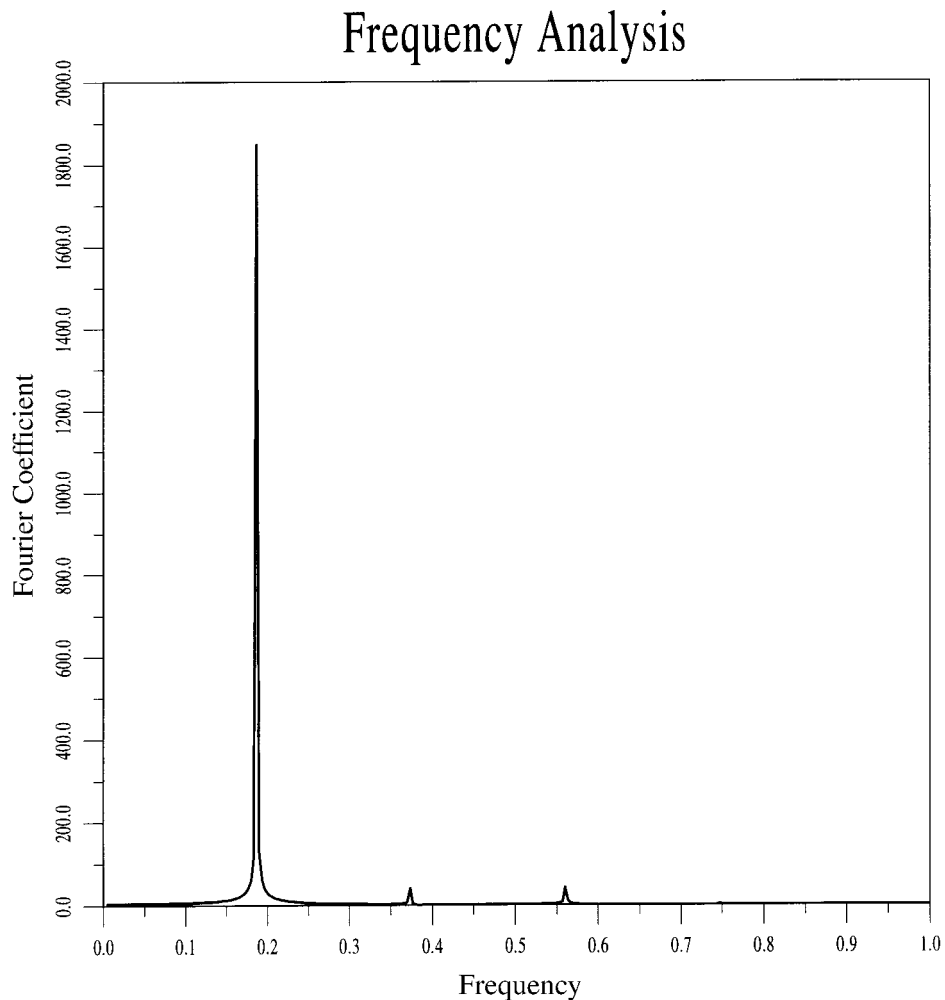

Figure 12. Flow past a cylinder, $Re = 100$, Fourier spectrum of the nodal velocity solution.

finite element implementations of the fractional-step method and the algorithm, using the $Q_1 P_0$ and the $Q_2 P_1$ element respectively, have been considered. The latter is particularly well-suited for these methods since it satisfies the discrete LBB condition.

Numerical results confirm the theoretical properties of these methods. First, a numerical convergence study is provided, which shows that first-order accuracy for the velocity can be obtained for the backward Euler case of the algorithm with only one correction per time step, which attains first-order accuracy for the pressure too. Also, a second-order method is found by setting the parameter of the algorithm to $1/2$ and iterating to convergence in each time step. The performance of the present scheme on standard benchmark tests for Navier–Stokes solvers, both for steady state and unsteady cases, has also been studied.

APPENDIX A

Given $f \in L^2(0, T; (H^{-1}(\Omega))^d)$, the weak form of Equations (1) and (2) consists of finding $u \in L^2(0, T; (H_0^1(\Omega))^d)$, and $p \in L^2(0, T; L_0^2(\Omega))$ such that:

$$\frac{\mathrm{d}}{\mathrm{d}t}(u(t), v) + ((u \cdot \nabla)u, v) + v((u, v)) - (\operatorname{div} v, p) = \langle f(t), v \rangle, \quad \forall v \in (H_0^1(\Omega))^d, \tag{38}$$

$$(\operatorname{div} u, q) = 0, \quad \forall q \in L_0^2(\Omega). \tag{39}$$

A solution of (38)–(39) exists, which is unique for v being sufficiently large [4]. In the two-dimensional case, the solution is always unique. These solutions are characterized by satisfying [4] $u \in L^2(0, T; V)$ and

$$\frac{\mathrm{d}}{\mathrm{d}t}(u(t), v) + ((u(t) \cdot \nabla)u(t), v) + v((u(t), v)) = \langle f(t), v \rangle, \quad \forall v \in V. \tag{40}$$

Assume $f \in L^2(0, T; (L^2(\Omega))^d)$, call $k = \Delta t$ and consider the scheme (4) and (6) with $\theta = 1$. It can be written in variational form as

(I) Find $u^{n+1/2} \in (H_0^1(\Omega))^d$ such that

$$\left(\frac{u^{n+1/2} - u^n}{k}, v \right) + v((u^{n+1/2}, v)) + c(u^n, u^{n+1/2}, v) = (\bar{f}^n, v), \quad \forall v \in (H_0^1(\Omega))^d. \tag{41}$$

(II) Find $u^{n+1} \in (H_0^1(\Omega))^d$ and $p^{n+1} \in (L_0^2(\Omega))^d$ such that

$$\left(\frac{u^{n+1} - u^{n+1/2}}{k}, v \right) + v((u^{n+1} - u^{n+1/2}, v)) + b(v, p^{n+1}) = 0, \quad \forall v \in (H_0^1(\Omega))^d, \tag{42}$$

$$b(u^{n+1}, q) = 0, \quad \forall q \in L_0^2(\Omega). \tag{43}$$

Then, one has:

Lemma 1
A priori estimate

$$|u^N|^2 + \sum_{n=0}^{N-1} (|u^{n+1} - u^{n+1/2}|^2 + |u^{n+1/2} - u^n|^2) + kv \sum_{n=0}^{N-1} \|u^{n+1}\|^2 + kv \sum_{n=0}^{N-1} \|u^{n+1}$$
$$- u^{n+1/2}\|^2 \leq d_2, \tag{44}$$

where $d_2 = |u^0|^2 + (d_0^2/v) \int_0^T |f(s)|^2 \, ds$ and d_0 was introduced in (3).

Proof

The proof is similar to that of Lemma 7.1.2 in [4].   □

Notice the last term appearing in the left-hand-side of (44), which is not present in [4].

Lemma 2

For every $m = 0, \ldots, N - 1$:

1. $|u^{m+i/2}|^2 \leq d_2, \quad i = 1, 2.$
2. $k \|u^{m+1/2}\|^2 \leq d_2/v.$
3. $\Sigma_{n=0}^{N-1} |u^{n+1} - u^{n+1/2}|^2 \leq d_2.$
4. $\Sigma_{n=0}^{N-1} |u^{n+1/2} - u^n|^2 \leq d_2.$
5. $k \Sigma_{n=0}^{N-1} \|u^{n+1} - u^{n+1/2}\|^2 \leq d_2/v.$
6. $k \Sigma_{n=0}^{N-1} \|u^{n+1}\|^2 \leq d_2/v.$

Proof

The proof, again, is similar to that of [4].   □

Notice that the bound 5 was not obtained in [4]. The approximating functions u_k^i and u_k defined in Section 4 satisfy, for decreasing k:

Lemma 3

1. u_k^i and u_k are bounded in $L^\infty(0, T; (L^2(\Omega))^d)$, $i = 1, 2, 3$.
2. u_k^i and u_k are bounded in $L^2(0, T; (H_0^1(\Omega))^d)$, $i = 1, 2, 3$.
3. $(u_k^2 - u_k^1)$ and $(u_k^2 - u_k^3)$ are bounded in $L^2(0, T; (H_0^1(\Omega))^d)$.

Proof

These results are a consequence of Lemma 2 and the definitions of the functions.   □

The main novelty with respect to [4] is now the boundedness of u_k^2 and u_k in $L^2(0, T; (H_0^1(\Omega))^d)$, together with that of the differences $(u_k^2 - u_k^1)$ and $(u_k^2 - u_k^3)$. Moreover

Lemma 4

1. $\|u_k^2 - u_k^1\|_{L^2(0, T; (L^2(\Omega))^d)} \leq \sqrt{kd_2}.$
2. $\|u_k^2 - u_k^3\|_{L^2(0, T; (L^2(\Omega))^d)} \leq \sqrt{4kd_2}.$
3. $\|u_k - u_k^2\|_{L^2(0, T; (L^2(\Omega))^d)} \leq \sqrt{4kd_2/3}.$

Proof

Part 1 follows from Lemma 2, part 3; 2 results from Lemma 2, parts 3 and 4 and the triangle inequality. Finally, 3 is a consequence of the definition of u_k and Lemma 2, parts 3 and 4. □

Lemma 5

$$\frac{\mathrm{d}}{\mathrm{d}t}(u_k(t), v) = -v((u_k^2(t), v)) - c(u_k^3(t), u_k^1(t), v) + (f_k(t), v) \equiv \langle g_k(t), v \rangle,$$

$$\forall v \in V, \quad \forall t \in (0, T), \tag{45}$$

with g_k bounded in $L^2(0, T; V')$. (For the definition of f_k, see [4].) In particular, u_k is a.e. equal to a continuous function from $[0, T]$ into V.

Proof

By adding (41) and (42), one gets:

$$\left(\frac{u^{n+1}-u^n}{k}, v\right) + v((u^{n+1}, v)) + c(u^n, u^{n+1/2}, v) = (\bar{f}^n, v), \quad \forall v \in (H_0^1(\Omega))^d,$$

so that (45) follows from the above definitions. Besides

$$\|g_k(t)\|_{V'} \le v\|u_k^2(t)\| + C\|u_k^3(t)\|\|u_k^1(t)\| + |f_k(t)|,$$

where $C > 0$ is a constant related to the continuity of the trilinear form c; the remaining statements are a consequent of Lemma 3 and Lemma III.1.1 of [4]. □

Proof of the theorem

Since u_k^i ($i = 1, 2, 3$) and $u_{k'}$ are bounded in $L^\infty(0, T; (L^2(\Omega))^d)$ there exists a subsequence k' (which can be taken the same for all four sequences) and u^i ($i = 1, 2, 3$), $u^* \in L^\infty(0, T; (L^2(\Omega))^d)$ such that:

$u_{k'}^i \to u^i$ in $L^\infty(0, T; (L^2(\Omega))^d)$ weak-star ($i = 1, 2, 3$)

$u_{k'} \to u^*$ in $L^\infty(0, T; (L^2(\Omega))^d)$ weak-star.

Since $u_{k'}^i$ ($i = 1, 2, 3$) and $u_{k'}$ are bounded in $L^2(0, T; (H_0^1(\Omega))^d)$, there exists a subsequence of k' (which is also denoted by k') such that:

$u_{k'}^i \to u^i$ in $L^2(0, T; (H_0^1(\Omega))^d)$ weakly ($i = 1, 2, 3$)

$u_{k'} \to u^*$ in $L^2(0, T; (H_0^1(\Omega))^d)$ weakly.

This convergence also holds in $L^2(0, T; (L^2(\Omega))^d)$. Since, by Lemma 4

$$(u_{k'}^2 - u_{k'}^3), \ (u_{k'}^2 - u_{k'}^1), \ (u_{k'}^2 - u_{k'}) \to 0 \text{ in } L^2(0, T; (L^2(\Omega))^d) \quad \text{strongly},$$

it must be $u^1 = u^2 = u^3 = u^*$.

Since $u_{k'}^2 \in L^\infty(0, T; H) \cap L^2(0, T; V)$, one has that $u^*(t) \in V$ a.e. in $(0, T)$, and $u^* \in L^\infty(0, T; H) \cap L^2(0, T; V)$.

The proof of strong convergence in $L^2(\Omega \times (0, T))$ is the same as in [4], and is therefore omitted. It only remains to show that u^* is a solution of (1). The same argument as in [4] is used, so that the convergence results already proved imply, by taking (45) to the limit when k' tends to 0, that:

$$\frac{d}{dt}(u^*, v) + v((u^*, v)) + c(u^*, u^*, v) = (f, v), \quad \forall v \in V,$$

in distribution sense in $(0, T)$, i.e. u^* satisfies (40). This, in turn, implies [4] that $du^*/dt \in L^1(0, T; V^1)$, $u^*(0) = u^0$ weakly in V and u^* is a.e. equal to a continuous function from $(0, T)$ into V. These results ensure that u^* is a weak solution of (1), and the theorem is thus proved. □

The proof of the corollary is a consequence of the uniqueness of the solution u in the two-dimensional case.

REFERENCES

1. A.J. Chorin, 'Numerical solution of the Navier–Stokes equations', *Math. Comput.*, **22**, 745–762 (1968).
2. R. Temann, 'Sur l'approximation de la solution des équations de Navier–Stokes par la méthode de pas fractionaires (I)', *Arch. Rac. Mech. Anal.*, **32**, 135–153 (1969).

3. N.N. Yanenko, *The Method of Fractional-Steps*, Springer, Berlin, 1971.
4. R. Temam, *Navier–Stokes Equations. Theory and Numerical Analysis*, North-Holland, Amsterdam, 3rd. edn., 1984.
5. A. Kovacs and M. Kawahara, 'A finite element scheme based on the velocity correction method for the solution of the time-dependent incompressible Navier–Stokes equations', *Int. J. Numer. Methods Fluids*, **13**, 403–423 (1991).
6. J. Blair Perot, 'An analysis of the fractional-step projection method', *J. Comput. Phys.*, **108**, 51–58 (1993).
7. J.K. Dukovicz and A.S. Dvinsky, 'Approximate factorization as a high-order splitting for the implicit incompressible flow equations', *J. Comput. Phys.*, **102**, 336–347 (1992).
8. L. Quartapelle, 'Numerical solution of the incompressible Navier–Stokes equations', *International Series in Numerical Mathematics*, vol. 113, Birkhäuser, Basel, 1993.
9. P.M. Gresho, 'On the theory of semi-implicit projection methods for viscous incompressible flow and its implementation via a finite element method that also introduces a nearly consistent mass matrix. Part I: theory', *Int. J. Numer. Methods Fluids*, **11**, 587–620 (1990).
10. P.M. Gresho and R. Sani, 'On pressure boundary conditions for the incompressible Navier–Stokes equations', *Int. J. Numer. Methods Fluids*, **7**, 1111–1145 (1987).
11. S.A. Orzag, M. Israeli and M.O. Deville, 'Boundary conditions for incompressible flows', *J. Sci. Comput.*, **1**, 75–111 (1986).
12. R. Temam, 'Remark on the pressure boundary condition for the projection method', *Theor. Comput. Fluid Dyn.*, **3**, 181–184 (1991).
13. J.B. Bell, P. Colella and H.M. Glaz, 'A second-order projection method for the incompressible Navier–Stokes equations', *J. Comput. Phys.*, **85**, 257–283 (1989).
14. J. van Kan, 'A second-order-accurate pressure correction scheme for viscous incompressible flow', *SIAM J. Sci. Stat. Comp.*, **7**, 870–891 (1986).
15. J. Kim and P. Moin, 'Application of a fractional-step method to incompressible Navier–Stokes equations', *J. Comput. Phys.*, **59**, 308–323 (1985).
16. H. Le and P. Moin, 'An improvement of fractional-step methods for the incompressible Navier–Stokes equations', *J. Comput. Phys.*, **92**, 369–379 (1991).
17. J. Donea, S. Giuliani, H. Laval and L. Quartapelle, 'Finite element solution of the unsteady Navier–Stokes equations by a fractional-step method', *Comput. Methods Appl. Mech. Eng.*, **30**, 53–73 (1982).
18. P.M. Gresho and S.T. Chan, 'On the theory of semi-implicit projection methods for viscous incompressible flow and its implementation via a finite element method that also introduces a nearly consistent mass matrix. Part 2: implementation', *Int. J. Numer. Methods Fluids*, **11**, 621–659 (1990).
19. H. Laval and L. Quartapelle, 'A fractional-step Taylor–Galerkin method for unsteady incompressible flows', *Int. J. Numer. Methods Fluids*, **11**, 501–513 (1990).
20. R. Natarajan, 'A numerical method for incompressible viscous flow simulation', *J. Comput. Phys.*, **100**, 284–395 (1992).
21. J. Shen, 'Hopf bifurcation of the unsteady regularized driven cavity flow', *J. Comput. Phys.*, **95**, 228–245 (1991).
22. J. Blasco, R. Codina and A. Huerta, 'Error estimates for a fractional-step method for the incompressible Navier–Stokes equations', *CIMNE Report*, No. 121 (1997).
23. A.N. Brooks and T.J.R. Hughes, 'Streamline upwind Petrov–Galerkin formulations for convection dominated flows with particular emphasis on the incompressible Navier–Stokes equations', *Comput. Methods Appl. Mech. Eng.*, **32**, 199–259 (1982).
24. W.K. Liu and J. Gvildys, 'Fluid–structure interaction of tanks with an eccentric core barrel', *Comput. Methods Appl. Mech. Eng.*, **58**, 51–77 (1986).
25. V. Girault and P.A. Raviart, *Finite Element Approximation of the Navier–Stokes Equation*, Springer, New York, 1986.
26. J. Shen, 'On error estimates of projection methods for Navier–Stokes equations: first-order schemes', *SIAM J. Numer. Anal.*, **29**, 57–77 (1992).
27. O.A. Ladyzhenskaya, *The Mathematical Theory of Viscous Incompressible Flow*, Gordon and Breach, New York, 1969.
28. R. Glowinski, T.W. Pan and J. Periaux, 'A fictitious domain method for external incompressible viscous flow modeled by Navier–Stokes equations', *Comput. Methods Appl. Mech. Eng.*, **112**, 133–148 (1994).
29. E. Fernandez-Cara and M. Marin Beltrán, 'The convergence of two numerical schemes for the Navier–Stokes equations', *Numer. Math.*, **55**, 33–60 (1989).
30. F. Brezzi and M. Fortin, *Mixed and Hybrid Finite Element Methods*, Springer Series in Computational Mathematics 15, Springer, Berlin, 1991.
31. L. Kleiser and U. Shumann, 'Treatment of incompressibility and boundary conditions in 3D numerical spectral simulation of plane channel flows', in E.H. Hirschel (ed.), *Proc. 3rd GAMM Conference on Numerical Methods in Fluid Mechanics*, Vieweg, Braunschweig, 1980.
32. L. Quartapelle and M. Napolitano, 'Integral conditions for the pressure in the computation of incompressible viscous flows', *J. Comput. Phys.*, **62**, 340–348 (1986).
33. J. Blasco, R. Codina and A. Huerta, 'A fractional-step method for the incompressible Navier–Strokes equations related to a predictor–multicorrector algorithm', *Internal Report No 63*, International Center for Numerical Methods in Engineering, 55 pp., 1995.

34. B.F. Armaly, F. Durst, J.C.F. Pereira and B. Shönung, 'Experimental and theoretical investigation of backward-facing step flow', *J. Fluid Mech*., **127**, 473–496 (1983).
35. G.K. Despotis and S. Tsangaris, 'Fractional-step method for solution of incompressible Navier–Stokes equations on unstructured triangular meshes', *Int. J. Numer. Methods Fluids*, **20**, 1273–1288 (1995).
36. L.P. Franca and S.L. Frey, 'Stabilized finite element methods: II. The incompressible Navier–Stokes equations', *Comput. Methods Appl. Mech. Eng*., **99**, 209–233 (1992).
37. M.A. Behr, D. Hastreiter, S. Mittal and T.E. Tezduyar, 'Incompressible flow past a circular cylinder: dependence of the computed flow field on the location of the lateral boundaries', *Comput. Methods Appl. Mech. Eng*., **123**, 309–306 (1995).
38. M.S. Engel and M.-A. Jamnia, 'Transient flow past a circular cylinder: a benchmark solution', *Int. J. Numer. Methods Fluids*, **11**, 985–1000 (1990).
39. S.J. Sherwin and G.E. Karniadakis, 'A triangular spectral element method; application to the incompressible Navier–Stokes equations', *Comput. Methods Appl. Mech. Eng*., **123**, 189–229 (1995).
40. J.C. Simó and F. Armero, 'Unconditional stability and long-term behaviour of transient algorithms for the incompressible Navier–Stokes and Euler equations', *Comput. Methods Appl. Mech. Eng*., **111**, 111–154 (1994).
41. T. Tanahashi, H. Okanaga and T. Saito, 'GSMAC finite element method for unsteady incompressible Navier–Stokes equations at high Reynolds numbers', *Int. J. Numer. Methods Fluids*, **11**, 479–499 (1990).
42. T.E. Tezduyar, S. Mittal and R. Shih, 'Time-accurate incompressible flow computations with quadrilateral elements', *Comput. Methods Appl. Mech. Eng*., **87**, 363–384 (1991).